Available online at www.sciencedirect.com
ScienceDirect
Journal of Power Sources 179 (2008) 101–105
JOURNAL OF POWER SOURCES
www.elsevier.com/locate/jpowsour

Short communication

Improved surface proton conduction of yttrium-stabilized zirconia via acidic modifications

Hui Wang, Liping Li, Yong Yang, Guangshe Li *

State Key Laboratory of Structural Chemistry, Fujian Institute of Research on the Structure of Matter and Graduate School of Chinese Academy of Sciences, Fuzhou 350002, PR China

Received 9 November 2007; received in revised form 14 December 2007; accepted 14 December 2007
Available online 4 January 2008

Abstract

This work studied the acidic surface modifications on the conduction properties of yttrium-stabilized zirconia (YSZ) nanocrystals using sulfuric and phosphoric acid protonation techniques with an aim to discover suitable additives of the proton-conducting membranes for intermediate temperature operation. All YSZ nanostructures were hydrothermally prepared and the sample surfaces were modified with sulfate or phosphate groups by subsequently immersing the as-prepared samples into sulfuric or phosphoric acid. The obtained samples were characterized by X-ray diffraction, high-resolution transmission electron microscope, element analysis, infrared spectra, N_2 adsorption/desorption, and impedance spectroscopy. It was found that the samples exhibited a cubic fluorite structure with a grain size of 4.5 nm and a high surface area of 205 $m^2\,g^{-1}$. Proton conduction measurements showed that sulfate-modified samples had an apparently low proton conductivity, while the phosphate-modified ones exhibited a significant proton conductivity and improved thermal stability. These observations were explained by taking into account the grafted species and the amount of hydrated water.

Keywords: Yttrium-stabilized zirconia; Surface modification; Proton conductivity

1. Introduction

Polymer electrolyte membrane fuel cells (PEMFCs) are one of the most promising clean energy technologies for transportation and stationary applications [1,2]. Polyperfluorosulfonic acid (PFSA) membranes such as Nafion are currently widely used as the key proton-conducting electrolyte for low-temperature PEMFCs. To possess advantages such as faster electrode kinetics, greater tolerance to impurities in the fuel stream, and easier water-thermal management, PEMFCs have to be operated at intermediate temperatures between 100 and 300 °C [3,4]. Unfortunately, such PFSA membranes are unavailable because of the low thermal stability and decreased conductivity that occur at high temperatures. There have been considerable efforts to modify the PFSA membranes to achieve high-temperature operation. One promising route is to add inorganic additives to PFSA to form composites. Previous literature work has shown that PFSA membranes modified by silica and H_3PO_4 additives can retain water for high conductivity even at higher temperatures [5,6]. However, since silica is amorphous in nature, its chemical/hydrolytic stability during the fuel cell operation is still questionable [7]. Furthermore, the existence of free phosphoric acid will degrade the mechanical properties of the membranes [8]. An alterative solution is to anchor acid onto insoluble species such as hydrous zirconia, since hydrous zirconia has an intrinsic proton conduction, higher thermal stability, and therefore is an ideal candidate for acidic modification [2,9]. Hara and Miyayama [10] studied the proton conduction of zirconia and found that the surface sulfation gave rise to a high conductivity of 5×10^{-2} S cm^{-1} at 60–150 °C which is promising for higher temperature composite PEMFC. Nevertheless, the applications of sulfated zirconia are still limited by high dependence on the relative humidity [1,11]. Comparatively, phosphorized zirconia nanoparticles (40–60 nm) were reported to exhibit proton conductivity of the order of 10^{-3} S cm^{-1} and show a better stability against relative humidity [8,12]. Nevertheless, the proton conductivity as a function of temperatures was previously popularly ignored and the nature of relationships between grafted

* Corresponding author. Tel.: +86 591 83702122; fax: +86 591 83714946.
E-mail address: guangshe@fjirsm.ac.cn (G. Li).

0378-7753/$ – see front matter © 2007 Elsevier B.V. All rights reserved.
doi:10.1016/j.jpowsour.2007.12.092

species and proton conductivity is still unclear, putting huge uncertainties in property optimization of phosphorized zirconia nanoparticles as additives of PFSA membranes.

In this work, we addressed the thermal stability and temperature dependent proton conductivity of YSZ nanoparticles. First, we successfully prepared YSZ nanoparticles with high surface area by hydrothermal process. Second, we grafted different acid groups onto the sample surfaces with an aim to enhance the proton conduction in terms of a better grain-to-grain transfer and larger concentrations of ionizable OH groups on surfaces. Finally, the effects of grafted species, microstructure, and surface hydration on proton conductivity were investigated.

2. Experimental

Eight moles percent of yttrium-stabilized zirconia nanocrystals were prepared by a hydrothermal method according to the following procedure: given amounts of Y_2O_3 were dissolved in diluted HNO_3 and then the obtained clear solution was mixed with 0.5 M $ZrOCl_2$ solution. Amorphous hydrated ZrO_2 was precipitated by adding the obtained mixed solution into ammonia solution (5 wt%) under continuous stirring. The mixed solution was adjusted to pH 10.5, which was then filtered and washed with deionized water till the filtrate did not become turbid when 3 M $AgNO_3$ was added. Then, this precipitate along with 4 M NaOH solution was transferred to 25 mL vessels sealed by stainless steel, which was placed in an oven at 130 °C for 12 h. The products were collected after washing with distilled water till the pH of the filtrate was about 7, and then dried at 60 °C for 3 h.

Sulfated and phosphated YSZ were obtained by immersing one gram of the as-prepared zirconia into 2.5 M H_2SO_4 and H_3PO_4 solution at room temperature for 2 h, respectively. The obtained samples were filtered off and then dried at 110 °C for 12 h in an oven.

The structures of the samples were characterized by X-ray diffraction (XRD) on Rigaku D/MAX 2500 X-ray diffractometer using a copper target. The grain size was calculated with Scherrer formula: $D = 0.9\lambda/(\beta \cos\theta)$, where λ is the X-ray wavelength, β is the half-width at half maximum, and θ is the diffraction angle. The particle sizes and morphologies of samples were determined using transmission electron microscope (TEM) on a JEM-2010 apparatus with an acceleration voltage of 200 kV. Surface areas of the samples were measured using Brunauer–Emmett–Teller (BET) method by N_2 adsorption and desorption at 77 K in a Micromeritics ASAP 2020 system. Chemical compositions of the samples were investigated by elemental analysis on Vario EL III and Inductive Coupled Plasma Emission (ICP) spectrometer on Ultima 2. Infrared spectra of the samples were measured on a Perkin–Elmer IR spectrophotometer using a KBr pellet technique.

The samples were pressed uni-axially into pellets with 7 mm in diameter and 1–2 mm in thickness under a pressure of 300 MPa. Silver paste was painted onto the opposite sides of the pellets and dried at room temperature to form the electrodes. Conductivity was determined by the AC impedance method on Agilent 4284 A apparatus in the frequency range of 20 Hz to 1 MHz with an applied voltage of 1 V and 30–150 °C under dry N_2 atmosphere.

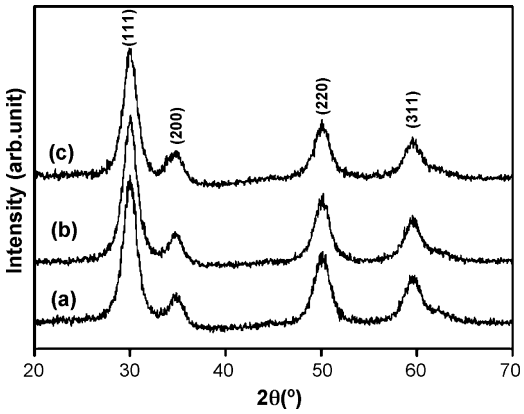

Fig. 1. XRD patterns of (a) as-prepared, (b) sulfate-modified YSZ, and (c) phosphate-modified YSZ.

3. Results and discussion

3.1. Synthesis of YSZ nanocrystals

XRD pattern of the as-prepared YSZ sample is shown in Fig. 1a. All diffraction peaks are indexed to the standard cubic fluorite structure (JCPDS. No. 89–6687). The diffraction peaks are obviously broadened, which indicates small particle size for the as-prepared YSZ. The mean particle size estimated by Scherrer formula for the most intense peak (1 1 1) is about 4.5 nm, which is confirmed by TEM micrographs (Fig. 2). It is also seen from Fig. 2 that the particles are homogeneously distributed in spherical shape and loosely agglomerated. The corresponding HRTEM image (inset of Fig. 2) clearly shows that the samples are highly crystalline. The interplanar spacing for (1 1 1) plane measured is 0.2882 nm, which is close to that obtained by XRD calculations.

The surface areas of the as-prepared YSZ nanocrystals were measured using BET method. The as-prepared samples show hysteresis loops at relatively high pressures, indicating a mesopore structure (Fig. 3). The pore size is distributed in the range

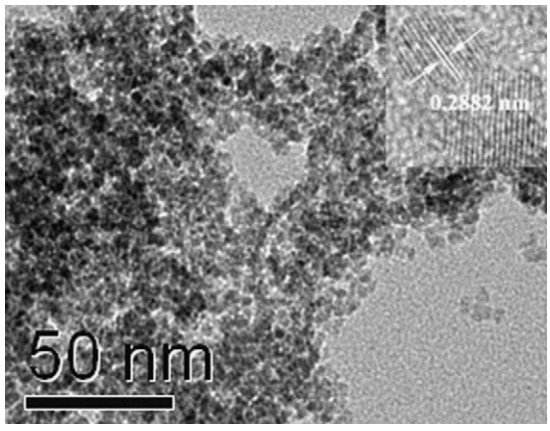

Fig. 2. TEM photo of the as-prepared YSZ nanoparticles. Inset: corresponding HRTEM image.

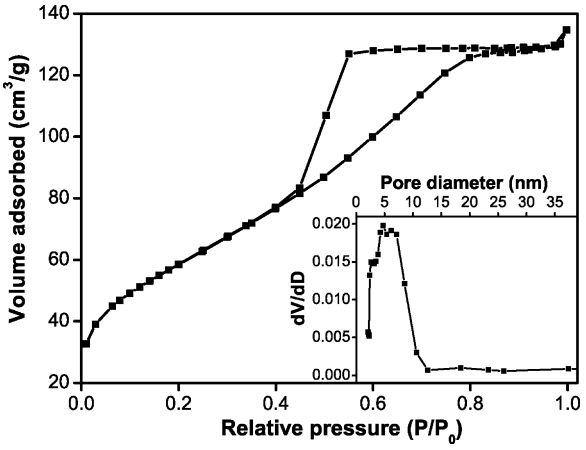

Fig. 3. N_2 adsorption/desorption isotherms of as-prepared YSZ. Inset: core size distribution.

of 3–10 nm (inset of Fig. 3). Interestingly, a high BET surface area of 205 $m^2\,g^{-1}$ is observed, which is significantly larger than that prepared by sol–gel or precipitation method [13].

The hydrated surface structure of YSZ was investigated by IR spectra. As shown in Fig. 4a, a strong broad absorption centered at 3415 cm^{-1} and two weak sharp absorption bands at 1630 and 1350 cm^{-1} are observed. The absorption band located around 3415 cm^{-1} is associated with the O–H stretching vibration of absorbed water and hydroxyl groups, while the absorption band at 1630 cm^{-1} is due to the bending mode of associated water [14]. The hydrated surface is highly reactive, which is indicated by the presence of the absorption band at 1350 cm^{-1} due to the formation of carbonate species by adsorbing atmospheric CO_2 [15]. The high surface area and a large amount of hydroxyl content on the surface make it a promising candidate for acidic modification.

3.2. Acidic surface modifications of YSZ nanostructures

Acidic surface modifications of YSZ nanostructures were investigated using sulfate and phosphate ions. The samples obtained after acidic surface modifications exhibited similar

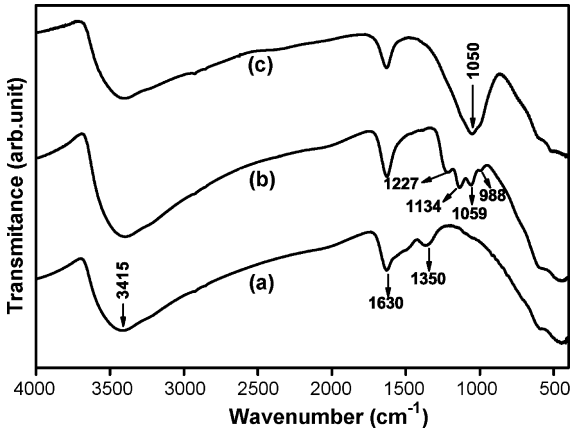

Fig. 4. IR spectra of (a) as-prepared YSZ, (b) sulfate-modified YSZ, and (c) phosphate-modified YSZ.

XRD patterns (Fig. 1b and c) to that of as-prepared YSZ in Fig.1a. Therefore, sulfate and phosphate modifications did not significantly alter the crystal structure or particle size. The surface terminations with sulfate and phosphate groups were confirmed by IR spectra. As shown in Fig. 4b, sulfated sample exhibited four absorptions at 1227, 1134, 1059, and 988 cm^{-1}, which were attributed to the asymmetric and symmetric stretching vibrations of S–O bonds for the inorganic chelating bidentate sulfate [16,17]. Therefore, Bronsted acid sites can be expected for the sulfated surfaces. On the other hand, the absorption band associated with the carbonate disappeared due to the reaction between carbonate and sulfuric acid. For phosphate-modified YSZ nanoparticles (Fig. 4c), the broad band observed in the range of 880–1425 cm^{-1} characterized the adsorption bands of coordinated phosphorous: HPO_4^{2-} (1000–1020 cm^{-1}), $H_2PO_4^-$ (1040–1090 cm^{-1}), and P–OH stretching band (1000–1020 cm^{-1}), indicating the presence of phosphate ions on surfaces [18]. From these IR spectra, it is demonstrated that the surfaces of YSZ nanocrystals were successfully modified with sulfate or phosphate ions. Elemental analysis shows that the as-prepared YSZ sample is compatible with a composition of $YSZ{\cdot}1.30H_2O{\cdot}0.04CO_2$, while the formula of samples after sulfate or phosphate modification can be expressed as $YSZ{\cdot}1.15H_2O{\cdot}0.08SO_3$ or $YSZ{\cdot}1.30H_2O{\cdot}0.02P_2O_5$ in sequence. Compared with the as-prepared YSZ, sulfated sample shows a decreased surface hydration, which is attributed to the reaction between surface OH groups and sulfate acid in terms of the following route:

$$2Zr-OH + H_2SO_4 = Zr_2-SO_4-2H_2O \quad (1)$$

This hypothesis is confirmed by our IR analysis where sulfate ions existed on the surfaces in the form of bidentately mode. Interestingly, phosphate-modified samples have similar hydration amount as that for the pure YSZ, which is associated with the polybasic acid nature of the phosphate acid. Every phosphate acid molecule has three hydroxyl groups, while only one or two of them reacted with surface of YSZ in terms of the following equation:

$$Zr-OH + H_3PO_4 = Zr-PO_2-(OH)_2+H_2O \quad (2)$$

$$2Zr-OH + H_3PO_4 = Zr_2-PO_3-OH + 2H_2O \quad (3)$$

The excess hydroxyl groups partially compensate the OH groups that were lost in the reaction. So, the surface hydration amount did not change obviously with the surface acidic modifications, though the distinct surface hydration and acid groups might have impacts on the proton conduction of the YSZ nanoparticles.

3.3. Optimized surface proton conduction of YSZ nanostructures via acidic modification

Fig. 5 shows the impedance curves of as-prepared YSZ as well as the sulfate and phosphate modified YSZ that were measured at 80 °C. A semicircle and a spike are observed in the whole frequency range, which are associated with the total resistance of proton conduction and electrode polariza-

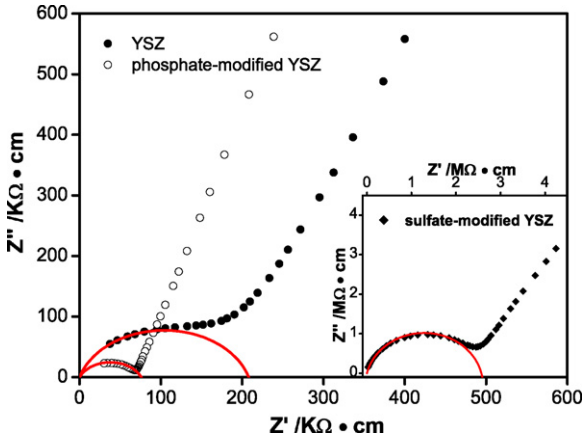

Fig. 5. AC impedance spectra for as-prepared YSZ (solid circle) and phosphate-modified (open circle) and sulfate-modified sample (inset) measured at 80 °C.

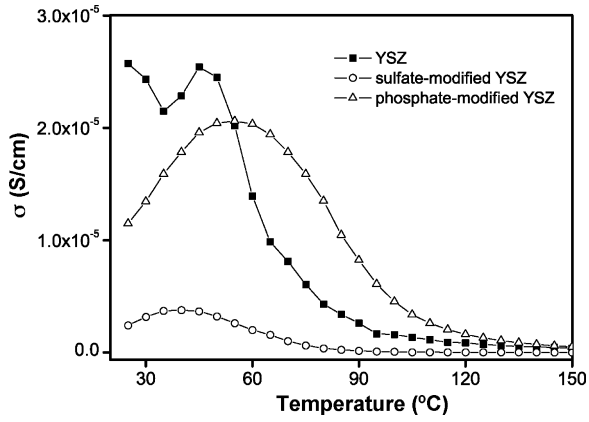

Fig. 6. Temperature dependence of the conductivity for as-prepared YSZ, sulfate-modified YSZ, and phosphate-modified YSZ.

tion, respectively [11]. The phosphate-modified samples give a significant proton conductivity of 1.35×10^{-5} S cm^{-1} at 80 °C, which is lower than that of 7.5×10^{-5} S cm^{-1} for hydration SnO_2 nanoparticles [3], but is several times larger than that of 4.32×10^{-6} S cm^{-1} for the pre-modified YSZ nanoparticles or that of 2.8×10^{-6} S cm^{-1} reported for zirconium phosphate under the similar measurement conditions [19]. In comparison with the phosphate-modified samples, the conductivity of sulfate-modified samples is low at 3.87×10^{-7} S cm^{-1}, which is still larger than that of 1.0×10^{-8} S cm^{-1} reported for sulfated ZrO_2 under the measurement conditions of 20 °C and low relative humidity of 19% [8].

Temperature dependences of the proton conductivity for the as-prepared materials are shown in Fig. 6. It is seen that when the temperature was increased from 45 to 150 °C, the proton conductivity of as-prepared YSZ samples decreased monotonously from 2.5×10^{-5} to 4×10^{-7} S cm^{-1}. While upon surface modification with phosphate ions, the samples exhibited a high proton conductivity and good thermal stability, especially in the temperature range from 25 to 85 °C. Comparatively, sulfated YSZ sample showed a best stability against temperature, however, the proton conductivity decreased greatly to less than 4×10^{-6} S cm^{-1}.

The conduction mechanism may be understood in terms of the surface hydration and acidic modifications. First, the conduction behavior of the as-prepared YSZ could be of Grotthuss type [19], in which the proton conductivity depends on the ability of surface water molecules to rotate and participate. The decrease in conductivity with increasing temperature is therefore attributed to the water loss as well as the condensation of structural hydroxyl groups at high temperatures. Consequently, surface hydration layers could play a key role in determining the proton conduction, just as what is proposed in literature [3]. But that does not mean that the concentration of mobile protons proportionally increase with the amounts of hydrated water, since the majority of hydration water molecules are directly chemically bonded to the surface metal ions, and hence the proton conductivity could be impacted by the electronegativity of surface metal ions. Because the electronegativity values for Zr and Y are 1.33 and 1.22, respectively, which are smaller than that of 1.96 for Sn, the bond between Zr (Y) and O in hydroxyl groups has a weaker covalent character. Then the bond strength between H and O is stronger and the dissociation of H^+ becomes weakened, which explains the low conductivity of pre-modified YSZ nanoparticles in comparison with the hydrated SnO_2 nanoparticles under dry atmosphere [3].

With regards to the roles of the surface acidic modifications, the difference observed in proton conductivity is probably associated with the grafted species. In comparison with the sulfate ions, the presence of $H_2PO_4^-$ and HPO_4^{2-} ions for the phosphated sample will promote the proton conduction by providing free pendant P–OH groups that show two-fold functions: (1)

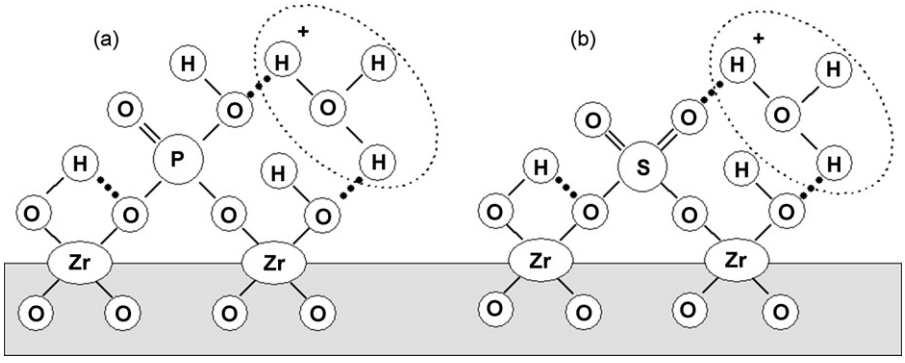

Fig. 7. Surface model of (a) phosphate-modified and (b) sulfate-modified YSZ.

attracting water molecules via hydrogen bond which increases the temperature as required for the removal of water from P–OH, and (2) donating protons to facilitate the charge transfer (Fig. 7a), which explains its good stability against temperature [20]. However, the surface water lost gradually with further increasing the temperature, which would induce insufficient water terminations to connect the pendant P–OH groups to give a continuous proton pathway. Consequently, phosphated sample exhibits low proton conductivity at high temperatures. Comparatively, for the sulfated YSZ nanoparticles, sulfated ions exist in the form of bidentately mode (Fig. 4), which could not provide free pendant S–OH group to promote the proton conduction. Besides these impacts, the loss of surface water could also cause a considerable decrease in proton conductivity. The strong hydrogen bond between sulfate and surface water might account for the high stability against temperature (Fig. 7b).

4. Conclusions

In this work, we have shown that nanometric YSZ with a high surface area is a good substrate for surface acid modification. When impregnated with sulfate groups, the sample exhibits a high stability against temperature due to the hydrogen bond between sulfate and surface water. Its proton conductivity decreased considerably for the low surface water content. Comparatively, modification with phosphate yielded a high proton conductivity. This phenomenon indicates that the presence of $H_2PO_4^-$ and HPO_4^{2-} ions can promote the proton transport by providing free pendant P–OH group to attract water and donate protons to facilitate the charge transfer. The hydrogen bond between P–OH and surface water may enable YSZ nanoparticles to show a good thermal stability as the additives of PFSA membranes for PEFC uses.

Acknowledgments

This work was supported by NSFC (No. 20671092, 20773132, 20771101), Science and Technology Program from Fujian Province (2005HZ01-1), Directional program (KJCX2-YW-M05), fjirsm (SZD08002) and a grant from Hundreds Youth Talents Program of CAS (Li GS)

References

[1] Y. Zhai, H. Zhang, J. Hu, B. Yi, J. Membr. Sci. 280 (2006) 148.
[2] M. Helen, B. Viswanathan, S.S. Murthy, J. Power Sources 163 (2006) 433.
[3] S. Hara, S. Takano, M. Miyayama, J. Phys. Chem. B. 108 (2004) 5634.
[4] Q. Li, R. He, J.O. Jensen, N.J. Bjerrum, Chem. Mater. 15 (2003) 4896.
[5] V.G. Ponomareva, V.A. Tarnopol'skii, E.B. Burgina, A.B. Yaroslavtsev, Russ. J. Inorg. Chem. 48 (2003) 955.
[6] K.D. Kreuer, S.J. Paddison, E. Spohr, M. Schuster, Chem. Rev. 104 (2004) 4637.
[7] G.M. Anilkumar, S. Nakazawa, T. Okubo, T. Yamaguchi, Electrochem. Comm. 8 (2006) 133.
[8] D. Carrière, M. Moreau, K. Lhalil, P. Barboux, J.P. Boilot, Solid State Ionics 162–163 (2003) 185.
[9] E.Yu. Voropaeva, I.A. Stenina, A.B. Yaroslavtsev, Russ. J. Inorg. Chem. 52 (2007) 1.
[10] S. Hara, M. Miyayama, Solid State Ionics 168 (2004) 111.
[11] H. Wang, X. Qiu, L. Li, G. Li, Chem. Lett. 36 (2007) 1132.
[12] G. Vaivars, J. Shan, G. Gericke, V. Linkov, Appl. Organomet. Chem. 19 (2005) 1096.
[13] J. Hu, Y. Cao, J. Deng, Chem. Lett. 5 (2001) 398.
[14] Y. Gao, Y. Masuda, H. Ohta, K. Koumoto, Chem. Mater. 16 (2004) 2615.
[15] K. Pokrovski, K.T. Jung, A.T. Bell, Langmuir 17 (2001) 4297.
[16] M.K. Mishra, B. Tyagi, R.V. Jasra, Ind. Eng. Chem. Res. 42 (2003) 5727.
[17] T. Yamaguchi, T. Jin, K. Tanabe, J. Phys. Chem. 90 (1986) 3148.
[18] W.H.J. Hogarth, S.S. Muir, A.K. Whittaker, J.C.D. da Costa, J. Drennan, G.Q. Lu, Solid State Ionics 177 (2007) 3389.
[19] R. Thakkar, H. Patel, U. Chudasama, Bull. Mater. Sci. 30 (2007) 205.
[20] M. Kato, S. Katayama, W. Sakamoto, T. Yogo, Electrochim. Acta 52 (2007) 5924.